Eur. J. Mineral.
2015, **27**, 417–426
Published online 27 February 2015

Ferro-pedrizite, $NaLi_2(Fe^{2+}{}_2Al_2Li)Si_8O_{22}(OH)_2$, a new amphibole-supergroup mineral from the Sutlug pegmatite, Tyva Republic, Russia

SERGEY I. KONOVALENKO[1], SERGEY A. ANANYEV[2], NIKITA V. CHUKANOV[3,*], SERGEY M. AKSENOV[4,5], RAMIZA K. RASTSVETAEVA[4], ANATOLIY I. BAKHTIN[6], ANATOLIY G. NIKOLAEV[6], RAMIL R. GAINOV[6,7,8], FARIT G. VAGIZOV[6], ANATOLIY N. SAPOZHNIKOV[9], DMITRIY I. BELAKOVSKIY[10], YANA V. BYCHKOVA[11], GÖSTAR KLINGELHÖFER[7] and MATHIAS BLUMERS[7]

[1] Tomsk State University, 36 Lenina pr., Tomsk, 634050 Russia
[2] Siberian Federal University, 79 Svobodny, Krasnoyarsk, 660041 Russia
[3] Institute of Problems of Chemical Physics, Russian Academy of Sciences, Chernogolovka, Moscow Region 142432, Russia
*Corresponding author, e-mail: chukanov@icp.ac.ru
[4] Institute of Crystallography, Russian Academy of Sciences, Leninskii Prospekt 59, Moscow 119333, Russia
[5] Department of Crystallography, St Petersburg State University, University Embankment 7/9, 199034 St Petersburg, Russia
[6] Kazan Federal University, Kremlyovskaya street 18, Kazan, 420008, Russia
[7] Johannes Gutenberg Universität Mainz, Staudingerweg 9, 55099 Mainz, Germany
[8] Helmholtz-Zentrum Berlin für Materialien und Energie, Hahn-Meitner Platz 1, 14109 Berlin, Germany
[9] A.P. Vinogradov Institute of Geochemistry, Siberian Branch of the Academy of Sciences, 1a Favorssky St., Irkutsk, 664033, Russia
[10] Fersman Mineralogical Museum of the Russian Academy of Sciences, Leninskiy Prospekt 18–2, Moscow, 119071, Russia
[11] Institute of Geology of Ore Deposits, Petrography, Mineralogy and Geochemistry, Russian Academy of Sciences, Staromonetny per. 35, Moscow, 119017, Russia

Abstract: Ferro-pedrizite, a new amphibole-supergroup mineral was discovered in the Sutlug pegmatite occurrence situated in the Targi River Basin, Tyva Republic, Eastern Sibera, Russia. The associated minerals are quartz, albite, microcline, spodumene, cassiterite, beryl, columbite-(Mn), fergusonite-β-(Y), fluorapatite, schorl, trilithionite and fluorite. Ferro-pedrizite forms dark grey-blue to violet-blue acicular and long prismatic crystals up to 2 × 5 × 50 mm and their aggregates. D_{meas} = 3.16(1) g/cm^3 (by hydrostatic weighing), 3.13(1) g/cm^3 (by flotation in heavy liquids); D_{calc} = 3.135 g/cm^3. Ferro-pedrizite is optically biaxial (–), α = 1.614(3), β = 1.638(3), γ = 1.653(3), $2V_{meas}$ = 75(5)°, $2V_{calc}$ = 76°. The infrared spectrum is given. The chemical composition is (EDS-mode electron microprobe, the ratio Fe^{2+}:Fe^{3+} by Mössbauer data, Li by ICP-MS, H_2O by gas chromatography of ignition products, F by wet analysis, wt. %): Li_2O 4.67, Na_2O 2.54, K_2O 0.13, MgO 4.48, CaO 0.29, MnO 0.59, FeO 9.06, Al_2O_3 13.13, Fe_2O_3 4.60, SiO_2 57.59, F 1.15, H_2O 1.50, -O = F –0.48, total 99.25. The empirical formula based on 24 anions is: $(Na_{0.60}K_{0.02})_{\sum 0.62}(Li_{1.89}Na_{0.07}Ca_{0.04})_{\sum 2.00}(Fe^{2+}{}_{1.03}Mg_{0.90}Mn^{2+}{}_{0.07}Al_{1.88}Fe^{3+}{}_{0.47}Li_{0.65})_{\sum 5.00}[(Si_{7.79}Al_{0.21})_{\sum 8.00}O_{22}][(OH)_{1.36}F_{0.49}O_{0.15})]$. The simplified formula is $NaLi_2(Fe^{2+}{}_2Al_2Li)Si_8O_{22}(OH)_2$. Ferro-pedrizite is monoclinic, *C*2/*m*, *a* = 9.3716(4), *b* = 17.649(1), *c* = 5.2800(6) Å, β = 102.22(1)°, *V* = 853.5(1) Å^3, *Z* = 2. The structure has been refined to R_{obs} = 3.9 % (4843 $I > 2\sigma I$). A twinning model was introduced into the refinement through the matrix [–1 0 0/0–1 0/–0.7516 0 1] with the ratio of two twin components of 0.681(3)/0.319(3). The strongest lines of the powder X-ray diffraction pattern [*d*, Å (*I*, %) (*hkl*)] are: 8.147 (52) (110), 4.420 (22), (040), 3.009 (100) (310), 2.7102 (28) (330), 2.6865 (29) (151), 2.6236 (21) (461). Type material is deposited in the Mineralogical Museum of the Tomsk State University, Tomsk, Russia.

Key-words: ferro-pedrizite; new mineral; amphibole supergroup; lithium amphibole; Sutlug pegmatite; crystal structure; Mössbauer.

Introduction

The general crystal-chemical formula of amphiboles is $AB_2C_5(T_8O_{22})W_2$, where $A = \square$, Na, K, Ca, Pb; B = Na, Ca, Mn^{2+}, Fe^{2+}, Mg, Li; C = Mg, Al, Li, Fe^{2+}, Fe^{3+}, Mn^{2+}, Mn^{3+}, Ti^{4+}; T = Si, Al, Ti^{4+}, Be; W = OH, F, Cl, O. Here C denotes the group of cations occurring at the [6-fold] coordinated sites $M(1) + M(2) + M(3)$. This terminology is the

DOI: 10.1127/ejm/2015/0027-2438
0935-1221/15/0027-2438 $ 4.50

one suggested by Hawthorne *et al.* (2012) for monoclinic *C*2/*m* amphiboles. The subgroup of lithium amphiboles is defined by $^{B}(Na + Li)/\Sigma B \geq 0.75$, $^{B}Li/\Sigma B > {}^{B}Na/\Sigma B$. The simplified general formula of amphiboles with the root-name ''pedrizite'' is $ALi_2C_5(Si_8O_{22})W_2$, where A is either Na or K (potassic-), C_5 is either Mg_2Al_2Li (pedrizite), $Fe^{2+}{}_2Al_2Li$ (ferro-pedrizite), $Mg_2Fe^{3+}{}_2Li$ (ferri-pedrizite), or $Fe^{2+}{}_2Fe^{3+}{}_2Li$ (ferro-ferri-pedrizite); W is OH, F (fluoro-) or Cl (chloro-). The distribution of bivalent and trivalent cations between *C*-sites is not a part of the definition of mineral species belonging to this subgroup (Hawthorne *et al.*, 2012).

This paper describes a new member of the lithium amphibole subgroup, ferro-pedrizite, $NaLi_2(Fe^{2+}{}_2Al_2Li)Si_8O_{22}(OH)_2$. The type material was collected in the end of the 20th century at the exocontact of lithium granite pegmatite at the Sutlug occurrence, Tyva Republic, Russia in the course of the study of spodumene pegmatites of the Sangilen Upland, in the southeast of Tyva. Ferro-fluoro-pedrizite, the F-dominant analogue of ferro-pedrizite, was described earlier as a new mineral from the same area (under the name ''fluoro-sodic-ferropedrizite'' suggested by the rules in force at that time), at the endocontact of a pegmatite body with country rocks near a diabase dike (Oberti *et al.*, 2009).

Ferro-pedrizite has been approved by the IMA Commission on New Minerals, Nomenclature and Classification (IMA no. 2014–037). The type specimen is deposited in the Mineralogical Museum of the Tomsk State University, Tomsk, 634050 Russia, with the registration number 19116.

Geological setting and occurrence

The Sutlug occurrence (50°00'20'' N, 96°37'40'' E) is located on the left shore of the Sutlug Creek related to the Targi River basin; it is composed of 15 boudinaged veins of spodumene–microcline pegmatites, 0.5 to 11.5 m thick and up to 160 m long, developed in partially bituminous, metasomatically altered marbles. This occurrence was discovered at the end of the 1960s in the course of prospecting of rare-metal pegmatites in the region. It is located in the near-latitudinal, up to 150 km long South-Sangilen pegmatite belt controlled by a well-manifested tectonic lineament. More than ten occurrences (Khartinskoye, Kachikskoye, Tserigingolskoye, Ak-Adytskoye *etc*.) and one large industrial rare-metal deposit, Tastyg, are known within the belt in addition to the Sutlug occurrence (Konovalenko & Garmayeva, 2012). Pegmatites of the belt belong mainly to the spodumene type. They have no direct genetic relations with specific intrusive massifs but, because of their age (483–494 Ma), they are considered to be derivatives of Ordovician granites of the Kystaryssky complex (Kuznetsova & Shokalsky, 2011).

The Sutlug pegmatite occurrence is confined to an abrupt bend of the northern limb of an anticline fold and is controlled by a thick tectonic zone passing along the creek valley. Steeply dipping (< 75–$80°$) tabular pegmatite bodies occur conformably with hosting marbles. They show a weak zonal organization and a clear directional structure. The orientation of spodumene crystals is near-perpendicular to contacts and becomes chaotic in central parts of the thickest veins where microcline megacrysts (> 0.5 m) developed. In some pegmatite bodies, minor veinlets formed by random aggregates of acicular spodumene crystals are present. Their paragenesis is similar to that of the surrounding coarse-grained pegmatite, and they have diffuse limits. Accessory cassiterite, beryl, columbite-(Mn), fergusonite-beta-(Y), fluorapatite, schorl, lepidolite and fluorite are found in the veins in addition to rock-forming minerals (quartz, albite, microcline and spodumene).

Rocks with unusual mineral composition are developed within the tectonic zone to the north of the main area of concentration of spodumene veins. They compose a series of contiguous, steeply dipping veins, up to 1.5 m thick and several metres long, cross-cutting the hosting marbles. The mineral composition of the veins includes quartz, albite, microcline, diopside, lithium amphibole and, locally, spodumene. Muscovite, titanite, apatite and pyrite are present as accessory minerals. The thickest veins have a zonal structure, symmetric or asymmetric, with a fine-grained quartz–diopside–albite aggregate developed on their margins. Thin veinlets are generally composed of quartz–diopside–albite or diopside–albite. The lithium amphibole from this occurrence was considered to be holmquistite in the 20th century; it developed along the contacts of major veinlets, both in their endo- and exocontacts, but it is more typical for the exocontact where it locally forms monomineralic zones and veins.

Our observations show that amphibole is not a primary phase of the spodumene pegmatites. The mineral assemblage including ferro-pedrizite was formed during the metasomatic alteration of grey bituminous marbles and pegmatite veinlets cross-cutting them. This process was accompanied by the formation of thick zones of vesuvianite, wollastonite and diopside impregnation in marble. A diopside–albite rock, locally with quartz and accessory apatite and titanite, was formed in the endocontact zone of the pegmatite bodies. The formation of ferro-pedrizite, along with pyrite, completed the transformation of the endocontact zone of the veins, while ferro-fluoro-pedrizite was formed at the same time in the exocontact zone.

General appearance and physical properties

Ferro-pedrizite occurs as flattened subhedral acicular and long-prismatic crystals up to $50 \times 5 \times 2$ mm without distinct terminations and with a lens-like cross-section typical for amphiboles. The crystals form random, radial or subparallel aggregates (Fig. 1).

The major crystal forms are {110} prism and the {100} and {010} pinacoids. The {100} pinacoid planes commonly show thin longitudinal striations due to oscillatory

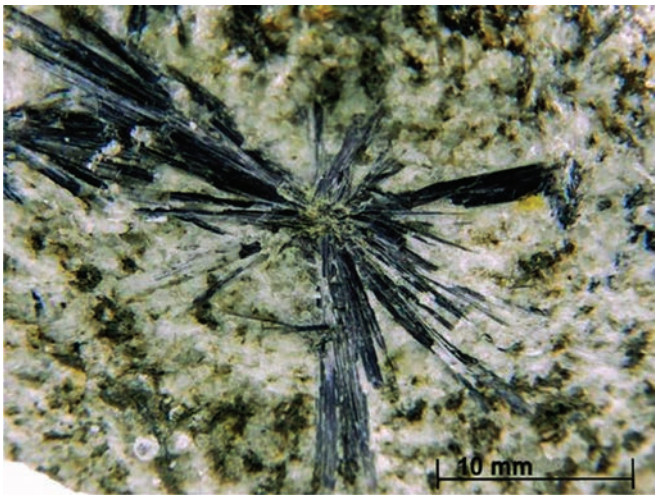

Fig. 1. Radial aggregates of ferro-pedrizite in albite–quartz matrix. (online version in colour)

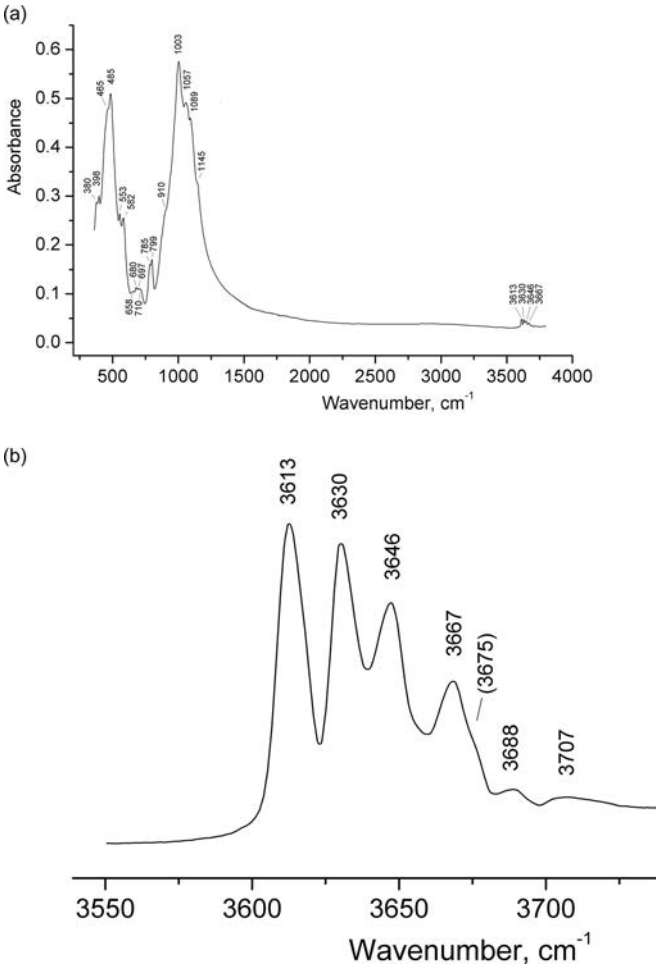

Fig. 2. Powder infrared absorption spectrum of ferro-pedrizite: (a) general view; (b) close-up in the region of O–H stretching vibrations.

combinations associated with the development of vicinal forms.

Ferro-pedrizite is intensely coloured, dark grey-blue to violet-blue; it shows no fluorescence under UV light. The streak is pale grey, the lustre is vitreous. Ferro-pedrizite is brittle, has a Mohs hardness of 6 and a splintery fracture; it has a perfect cleavage on (110) and a less perfect one on (001).

The density measured by flotation in heavy liquids (diiodomethane-ether mixtures) is 3.13(1) g/cm^3. The densities of the liquids have been measured using a density bottle. The density measured by hydrostatic weighing is 3.16(1) g/cm^3. The density calculated from the empirical formula is 3.138 g/cm^3.

Ferro-pedrizite is biaxial (–), $\alpha = 1.614(3)$, $\beta = 1.638(3)$, $\gamma = 1.653(3)$; $2V_{meas} = 75(5)^\circ$, $2V_{calc} = 76^\circ$. The orientation is: $Y = b$, $Z\wedge c = 3$–4°, $X\wedge a \approx 16^\circ$. Positive elongation is observed for the grains parallel to the planes {010} and (*YZ*). The dispersion of the optical axes is weak, $r < v$. A weak pleochroism is observed (colourless on *X* and pale lilac-grey on *Y* and *Z*). The absorption scheme is $Y \approx Z > X$.

Infrared, Mössbauer and optical (in the visible range) spectroscopy

The infrared absorption spectrum (Fig. 2) was obtained using a Bruker Optics ALPHA FTIR spectrometer, with 16 scans of the wavenumber range 360–3800 cm^{-1} and a resolution of 4 cm^{-1}. The powdered mineral was mixed with dry KBr and pelletized. The spectrum of an analogous pure KBr disk was subtracted from the overall spectrum.

The IR spectrum of ferro-pedrizite is similar to the IR spectra of other Al-poor lithium amphiboles (Chukanov, 2014). The bands in the ranges 550–600 and 3600–3750 cm^{-1} correspond to Li–O- and O–H-stretching vibrations, respectively. The assignment of other bands is as follows: the range from 900 to 1150 cm^{-1} corresponds to Si–O stretching vibrations; the bands with wavenumbers from 650 to 800 cm^{-1} can be assigned to O–Si–O and $M \cdots$ O–H bending vibrations (where $M = {}^{VI}$Al, Fe, Mg, Li); the bands below 600 cm^{-1} correspond to *M*–O stretching and Si–O–Si bending modes.

Numerous bands of O–H stretching vibrations (Fig. 2b) indicate the presence of hydroxyl groups having different local environments. In an amphibole with an empty *A* site, hydroxyl completes the octahedral coordination of the *M*(l) and *M*(3) sites by forming the apex of a flat pseudotrigonal pyramid, the base of which consists of two *M*(l) sites and one *M*(3) site (Mottana & Griffin, 1986).

The OH-stretching bands can be divided into two regions. The lower-frequency bands between 3680 and 3600 cm^{-1} are ascribed to OH groups adjacent to a vacant *A*-site, [*M*(1)*M*(1)*M*(3)]-OH-□, and the higher-frequency bands above 3680 cm^{-1} are ascribed to OH groups adjacent to a filled *A*-site, [*M*(1)*M*(1)*M*(3)]-OH-*A*, where *A* is occupied with Na or K (Ishida & Hawthorne, 2001). In particular, bands with the wavenumbers 3613–3614, 3624–3630, 3647 and 3662 have been assigned to ${}^{M(1)}Fe^{2+}{}^{M(1)}Fe^{2+}{}^{M(3)}Fe^{2+}$-OH-^{A}□,

$^{M(1)}Mg^{M(1)}Fe^{2+M(3)}Fe^{2+}$-OH–$^{A}\square$, $^{M(1)}Mg^{M(1)}Mg^{M(3)}Fe^{2+}$-OH–$^{A}\square$ and $^{M(1)}Mg^{M(1)}Mg^{M(3)}$Mg-OH–$^{A}\square$, respectively (Iezzi *et al.*, 2004; Della Ventura *et al.*, 2005). Based on this assignment, we can conclude that four analogous local situations correspond to the bands at 3613, 3630, 3646 and 3667 cm^{-1} present in the IR spectrum of ferro-pedrizite. The bands observed at 3675, 3688 and 3707 cm^{-1}, which must be assigned to the local configurations like $^{M(1)}Fe^{2+M(1)}Fe^{2+M(3)}Fe^{2+}$-OH–^{A}Na, $^{M(1)}Mg^{M(1)}Fe^{2+M(3)}Fe^{2+}$-OH–^{A}Na, or $^{M(1)}Mg^{M(1)}Mg^{M(3)}Fe^{2+}$-OH–^{A}Na, are weak. Although extinction coefficients of O–H stretching bands of OH groups coordinated by Na seem to be lower than those of OH groups attached to vacancy (Chukanov, 2014), this observation may indicate that Na^{+} cations are predominantly coordinated by F^{-} anions, and only a minor part of $^{A(m)}$Na is involved in the local configuration of the OH.

The room-temperature ^{57}Fe-Mössbauer experiments were carried out using a backscattering miniaturized (portative) Mössbauer spectrometer MIMOS-II (Klingelhoefer *et al.*, 2002; Gainov *et al.*, 2013, 2014) equipped with a radioactive cobalt source (^{57}Co). The remote backscattering mode of MIMOS was applied to prevent the possible destruction of the sample. This is important for the case of minerals that could change their properties during specific preparation for experiment. The Mössbauer spectrum was recorded in the constant acceleration mode. The calibration was made using α-Fe as reference absorber.

The Mössbauer spectrum of ferro-pedrizite (Fig. 3) can be interpreted as a superposition of four doublets. Two of them (the doublets 1 and 2 with isomer shifts 1.121 and 1.076 mm/s, quadrupole splitting 2.917 and 2.272 mm/s and relative areas 46.3 and 22.4 %, respectively) correspond to Fe^{2+}. Two other doublets (the doublets 3 and 4 with isomer shifts –0.059 and 0.082 mm/s, quadrupole splitting 0.361 and 0.995 mm/s and relative areas 25.5 and 5.8 %, respectively) correspond to Fe^{3+}. Consequently, the Fe^{2+}: Fe^{3+} ratio is 68.66: 31.34.

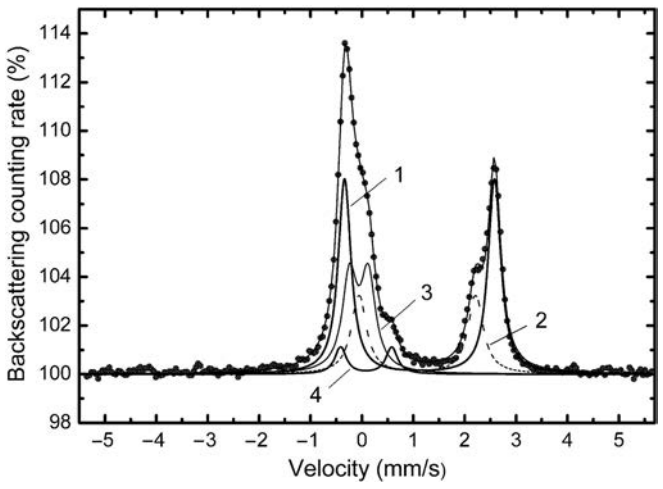

Fig. 3. Mössbauer spectrum of ferro-pedrizite obtained at room temperature (circles). Four doublets and their superposition are shown with curves.

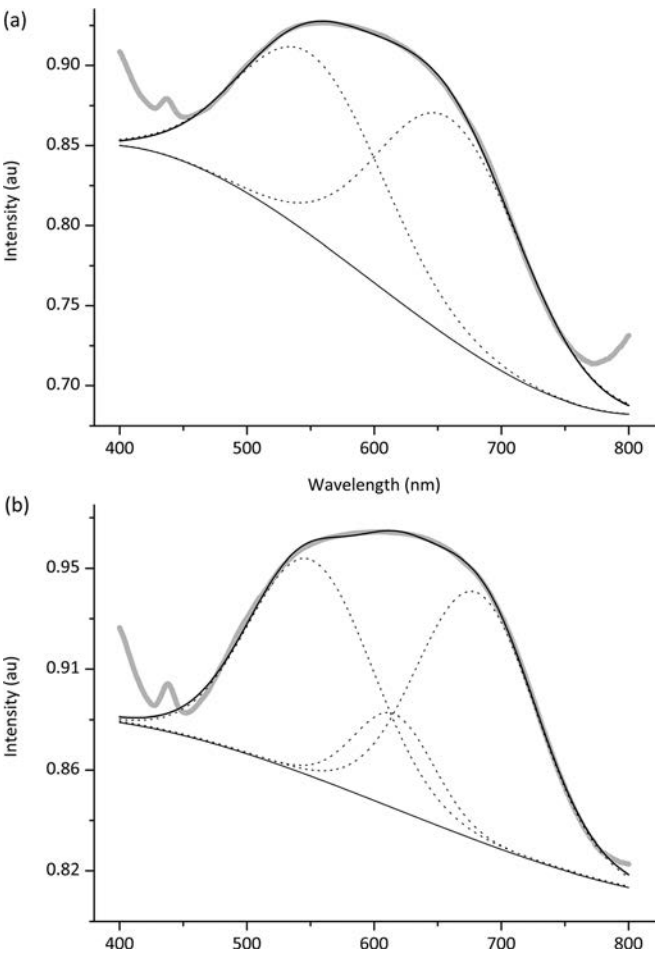

Fig. 4. Optical absorption spectra of ferro-pedrizite, obtained with the polarization $E \parallel c$ (a) and $E \perp c$ (b). (online version in colour)

The doublets 1 and 3 (with the total area 71.79 %) can be correlated with iron in $M(1)$ site which amounts to 69 % of all iron present in the mineral. Under this assumption, the ratio Fe^{2+}: Fe^{3+} in $M(1)$ is close to 46.28: 25.51. The doublets 2 and 3 can be correlated with Fe^{2+} in $M(3)$ and Fe^{3+} in $M(2)$ (23 % and 8 % of all iron present in the mineral, respectively).

The transmission-mode optical spectrum within the wavelength range 400–800 nm (Fig. 4) was obtained for a thin section using a MSFU microspectrometer. It is characterized by strong absorption in the 500 to 700 nm range corresponding to the $Fe^{2+} \rightarrow Fe^{3+}$ charge transfer (Bakhtin, 1978). Additionally, a weak narrow band corresponding to the spin-forbidden electronic transition in the $^{VI}Fe^{3+}$ ions is observed at 438 nm. The comparison of the spectra recorded with different light polarization ($E \parallel c$ and $E \perp c$) shows that the intense absorption of ferro-pedrizite in the 500–700 nm range is due to two and three broad overlapping absorption bands, respectively (Fig. 4). The spectrum obtained with the polarization $E \parallel c$ (Fig. 4a) is a superposition of two Gaussian components with the absorption maxima at 550 and 660 nm. The spectrum obtained with the polarization

Table 1. Chemical composition of ferro-pedrizite (mean of five point analyses).

Constituent	wt%	Range	SD	Probe standard
Li_2O	4.67			
Na_2O	2.54	2.43–2.67	0.08	Albite
K_2O	0.13	Bdl-0.23	0.10	Sanidine
MgO	4.48	4.27–4.64	0.17	Diopside
CaO	0.29	0.20–0.35	0.05	Wollastonite
MnO	0.59	0.43–0.65	0.09	$MnTiO_3$
FeO*	9.06			
Fe_2O_3*	4.60			
FeO_{total}	13.20	13.02–13.37	0.15	Fe_2O_3
Al_2O_3	13.13	12.80–13.46	0.28	Albite
SiO_2	57.59	57.25–57.91	0.28	SiO_2
F	1.15(1)			
H_2O	1.50(1)			
$-O = F$	−0.48			
Total	99.25			

Note: The SD values refer to the crystal for which the structure was investigated.
*The total iron content analysed using a microprobe and initially calculated as FeO was 13.20 wt%; it was apportioned between FeO and Fe_2O_3 on the basis of Mössbauer data.

$E\perp c$ (Fig. 4b) consists of three bands (at 550, 616 and 680 nm), which indicates the presence of three different adjacent pairs Fe^{2+}+Fe^{3+}. These specific features of the spectrum determine the colour of ferro-pedrizite and its pleochroism. Taking into account optical data, we can suppose that the mineral is colourless in the *X* direction because charge transfer takes place within *M* slabs, and not between *M* slabs (*i.e.* nearly parallel to *X*). The most probable charge-transfer pairs corresponding to the bands at 550 and 660–680 nm are $Fe^{3+}(M1)$–$Fe^{2+}(M3)$ and $Fe^{2+}(M1)$–$Fe^{3+}(M2)$. Additional component at 616 nm with the polarization $E\perp c$ can be assigned to the charge transfer in the pair $Fe^{3+}(M2)$–$Fe^{2+}(M3)$.

Chemical data

The majority of elements were analysed by means of an electron microprobe. Five point analyses were performed using the digital scanning electron microscopes Tescan VEGA-II XMU and VEGA-II XMU with energy-dispersive spectrometers (EDS) INCA Energy 450 and Energy 350. The analyses were carried out at an accelerating voltage of 20 kV; the current of absorbed electrons on a reference sample of cobalt was 510–520 pA and the electron beam diameter on the sample surface varied from 150 to 200 nm.

Lithium was analyzed by the ICP-MS method using a Thermo Fisher Scientific X Series II instrument. A hand-picked sample was dissolved in a mixture of concentrated aqueous HCl, HF and HNO_3 solutions. After total evaporation, 5 cm^3 of 0.5 M nitric acid was added, and the solution analysed by measuring the intensities of the lines corresponding to $m/e = 7$.

H_2O was determined by gas chromatography of products of the mineral ignition at 1200°C with a Vario Micro cubeanalyser (Elementar GmbH, Germany).

Since measurement of F using EDS is unreliable in such Fe-rich minerals, due to the overlap of F*Kα* and Fe*L* lines, the fluorine content was determined by wet chemical analysis. The analysis is based on titration of an acid solution of the mineral with an aqueous solution of thorium Arsenazo complex having a blue colour. The abatement of the blue colour was followed using a SF-46 spectrometer (LOMO Association, Russia).

Table 2. Powder X-ray diffraction data of ferro-pedrizite.

I_{rel}	d_{meas}, Å	I_{calc}*	d_{calc}, Å*	*hkl*	I_{rel}	d_{meas}, Å	I_{calc}*	d_{calc}, Å*	*hkl*
52	8.147	100	8.130	110	13	2.2884	1	2.2898	400
11	4.786	1	4.782	$11\bar{1}$	18	2.2461	20	2.2461	$35\bar{1}$
16	4.583	3	4.580	200	15	2.2082	2	2.2071	$42\bar{1}$
22	4.420	77	4.412	040	16	2.1987	19	2.1982	$31\bar{2}$
14	4.033	37	4.028	111	14	2.1533	12	2.1530	170
15	3.798	18	3.796	$13\bar{1}$	18	2.1388	24	2.1382	261
16	3.532	34	3.532	$22\bar{1}$	15	2.0702	9, 7	2.0733, 2.0685	332, $02\bar{2}$
18	3.385	38	3.384	131	16	1.9922	11	1.9922	351
18	3.181	3	3.176	240	13	1.9255	5	1.9271	$40\bar{2}$
100	3.009	79	3.008	310	15	1.9011	9	1.9002	421
17	2.9366	5	2.9362	221	13	1.8728	12	1.8728	242
16	2.8760	12	2.8775	$15\bar{1}$	17	1.8218	2	1.8220	510
28	2.7102	24	2.7099	330	14	1.7722	11	1.7720	191
29	2.6865	93	2.6852	151	14	1.7667	6	1.7649	0.10.0
15	2.6084	10	2.6095	$33\bar{1}$	14	1.7485	1	1.7490	530
13	2.5788	9	2.5801	002	14	1.7437	1	1.7434	371
15	2.5565	22	2.5555	061	15	1.6615	10	1.6624	$51\bar{2}$
19	2.4824	49	2.4841	$20\bar{2}$	21	1.6236	25	1.6229	461
13	2.4325	13	2.4309	171	15	1.5892	9	1.5887	480
14	2.3093	10	2.3092	350	15	1.5751	24	1.5747	$15\bar{3}$

Note: *Calculated from structural data.

Table 3. Crystallographic data and refinement parameters for ferro-pedrizite.

Crystal data	
Simplified formula	$NaLi_2(Fe^{2+}{}_2Al_2Li)Si_8O_{22}(OH)_2$
Absorption, μ (mm^{-1})	2.211
Density, D_x (g/cm^3)	3.125
Crystal system	Monoclinic
Space group	*C*2/*m*
a (Å)	9.3716(4)
b (Å)	17.649(1)
c (Å)	5.2800(6)
β (deg)	102.22(1)
V ($Å^3$)	853.5(1)
Z	2
Crystal size (mm)	0.15 × 0.18 × 0.20
Data collection	
Diffractometer	XCalibur Oxford Diffraction
Radiation; wavelength (Å)	Mo*K*α; 0.7107
Data collection method	ω
Temperature (K)	293
F(000)	791
Theta range for data collection (deg)	4.12 to 56.2
Index ranges	$-21 < h < 21, -39 < k < 41, -12 < l < 11$
Reflections collected	23602
Unique reflections/R_{int}	5541/5.84
Observed reflections ($I_{obs} > 2\sigma(I)$)	4843
Refinement	
Matrix of twinning	[–1 0 0/0–1 0/–0.7516 0 1]
Twin component ratio	0.681(3)/0.319(3)
Refinement method	Full matrix least square on *F* weight scheme:$w = 1/(\sigma^2F + 0.002025F^2)$
Goodness-of-fit on *F*	1.03
Final *R* indices	$R_1 = 3.91$; $wR_2 = 6.77$
$\Delta\rho_{min}/\Delta\rho_{max}$ ($e/Å^3$)	−0.92/1.92*

* Positive residual electron density is observed in the region of *Am*-site.

Note: $R_1 = \sum||F_{obs}|-|F_{calc}||/\sum|F_{obs}|$; $wR_2 = \{\sum[w(F_{obs}{}^2-F_{calc}{}^2)^2]/\sum[w(F_{obs}{}^2)^2]\}^{1/2}$;

GOF = $\{\sum[w(F_{obs}{}^2-F_{calc}{}^2)]/(n-p)\}^{1/2}$ where *n* is the number of reflections and *p* is the number of refined parameters.

The analytical data are given in Table 1. The contents of other elements with atomic numbers > 8 are below detection limits of the EDS-mode electron microprobe analysis.

The empirical formula (based on 24 anions) is $(Na_{0.60}K_{0.02})_{\sum 0.62}(Li_{1.89}Na_{0.07}Ca_{0.04})_{\sum 2.00}(Fe^{2+}{}_{1.03}Mg_{0.90}Mn^{2+}{}_{0.07}Al_{1.88}Fe^{3+}{}_{0.47}Li_{0.65})_{\sum 5.00}[(Si_{7.79}Al_{0.21})_{\sum 8.00}O_{22}][(OH)_{1.36}F_{0.49}O_{0.15})]$.

The simplified formula is $NaLi_2(Fe^{2+}{}_2Al_2Li)Si_8O_{22}(OH)_2$, which requires Li_2O 5.46, Na_2O 3.78, FeO 17.52, Al_2O_3 12.43, SiO_2 58.61, H_2O 2.20, total 100.00 wt%.

The Gladstone-Dale compatibility index is: $1–(K_p/K_c) = 0.030$ (''excellent'').

X-ray diffraction data and crystal structure

The powder X-ray diffraction data (Table 2) were collected by means of a Bruker D8 ADVANCE X-ray diffractometer using Cu*K*α radiation. The monoclinic unit-cell parameters refined from the powder data are: $a = 9.376(4)$, $b = 17.663(2)$, $c = 5.277(6)$ Å, $\beta = 102.22(1)^\circ$, $V = 854.1(1)$ $Å^3$.

Single-crystal X-ray studies were carried out with an Xcalibur Oxford Diffraction CCD diffractometer (Mo*K*a radiation). The data were reduced using CrysAlis software (Oxford Diffraction, 2009). The structure determination and refinement were carried out using the JANA2006 program package (Petricek *et al.*, 2006). Scattering curves for neutral atoms, together with anomalous dispersion corrections, were taken from *International Tables for X-Ray Crystallography* (Ibers & Hamilton, 1974). The initial model for the structure refinement was based on coordinates of the fluoro-pedrizite structure (Oberti *et al.*, 2005). Crystals of ferro-pedrizite were found to be twinned. A twinning model was introduced into the refinement through the matrix [–1 0 0/0–1 0/–0.7516 0 1] with the ratio of two twin components of 0.681(3)/0.319(3). The crystal structure was refined anisotropically to $R = 0.0391$ for 4843 unique reflections with $I > 2\sigma(I)$ (Tables 3–5; Figs. 5 and 6).

Table 4. Site coordinates, refined site-scattering values (e_{ref}, epfu) and atomic displacement parameters (U_{eq}, $Å^2$) for ferro-pedrizite.

Site	*x*	*y*	*z*	e_{ref}	U_{eq}	U_{11}	U_{22}	U_{33}	U_{12}	U_{13}	U_{23}
A(*m*)	0.0748(4)	0.5	0.1499(7)	7.0	0.030(1)	0.042(2)	0.019(1)	0.038(2)	0	0.027(1)	0
M(1)	0	0.0899(1)	0.5	19.7	0.0091(1)	0.0102(1)	0.0089(1)	0.0089(1)	0	0.0036(1)	0
M(2)	0	0.1799(1)	0	13.8	0.0064(1)	0.0065(1)	0.0061(1)	0.0068(1)	0	0.0018(1)	0
M(3)	0	0	0	11.0	0.0043(1)	0.0060(1)	0.0021(1)	0.0046(1)	0	0.0007(1)	0
M(4)	0	0.2580(2)	0.5	3.6	0.030(1)	0.020(1)	0.053(2)	0.018(1)	0	0.007(1)	0
T(1)	0.2847(1)	0.0879(1)	0.2783(1)		0.0055(1)	0.0065(1)	0.0046(1)	0.0056(1)	−0.0000(1)	0.0019(1)	−0.0001(1)
T(2)	0.2975(1)	0.1737(1)	0.7917(1)		0.0056(1)	0.0062(1)	0.0053(1)	0.0057(1)	0.0007(1)	0.0019(1)	0.0001(1)
O(1)	0.1089(1)	0.0945(1)	0.1978(1)		0.0072(1)	0.0060(1)	0.0076(1)	0.0082(2)	0.0000(1)	0.0018(1)	0.0001(1)
O(2)	0.3801(1)	0.1753(1)	0.7420(1)		0.0078(1)	0.0064(1)	0.0090(2)	0.0082(2)	0.0002(1)	0.0022(1)	−0.0006(1)
O(3)	0.1171(1)	0	0.6972(1)		0.0110(2)	0.0108(2)	0.0091(2)	0.0130(3)	0	0.0020(2)	0
O(4)	0.3776(1)	0.2532(1)	0.7904(1)		0.0098(1)	0.0105(2)	0.0075(2)	0.0110(2)	−0.0035(1)	0.0016(1)	0.0004(1)
O(5)	0.3582(1)	0.1291(1)	0.0650(1)		0.0110(1)	0.0080(2)	0.0154(2)	0.0100(2)	0.0001(1)	0.0026(1)	0.0065(2)
O(6)	0.3462(1)	0.1234(1)	0.5624(1)		0.0121(1)	0.0097(2)	0.0172(2)	0.0091(2)	0.0014(2)	0.0015(1)	−0.0063(2)
O(7)	0.3363(1)	0	0.2874(1)		0.0115(2)	0.0109(2)	0.0044(2)	0.0192(3)	0	0.0029(2)	0

Table 5. Interatomic distances (Å) in the structure of ferro-pedrizite.

A(*m*)	O(7)	2.492(4)	*M*(3)	O(1)	2.112(1) x4
	O(7)	2.615(4)		O(3)	2.122(1) x2
	O(6)	2.669(2) x2			<2.115>
	O(5)	2.678(2) x2			
	O(3)	2.829(4)	*M*(4)	O(2)	2.102(3) x2
	O(7)	2.911(4)		O(4)	2.110(1) x2
	O(5)	3.021(3) x2		O(6)	2.602(3) x2
		<2.758>		O(5)	3.118(2) x2
A(*m*)	*A*(*m*)	1.879(5)			<2.271>[6]
M(1)	O(1)	2.070(1) x2			<2.483>[8]
	O(3)	2.079(1) x2	*T*(1)	O(5)	1.613(1)
	O(2)	2.135(1) x2		O(6)	1.615(1)
		<2.095>		O(1)	1.616(1)
M(1)	*M*(2)	3.081(1)		O(7)	1.623(1)
$\Delta^{M(1)}$		1.884			<1.617>
M(2)	O(4)	1.843(1) x2	*T*(2)	O(4)	1.591(1)
	O(2)	1.942(1) x2		O(2)	1.629(1)
	O(1)	1.988(1) x2		O(5)	1.637(1)
		<1.924>		O(6)	1.642(1)
					<1.625>

Note: $\Delta = (1/6)\sum_{i=1-6}[(M\text{–O})_i - \langle M\text{–O}\rangle/\langle M\text{–O}\rangle] \times 10^4$.
Octahedron distortion $\Delta^{M(1)}$ as well as *M*(1)–*M*(2) distance are in a good agreement with the presence of an oxo component in ferro-pedrizite (Oberti *et al.*, 2007).

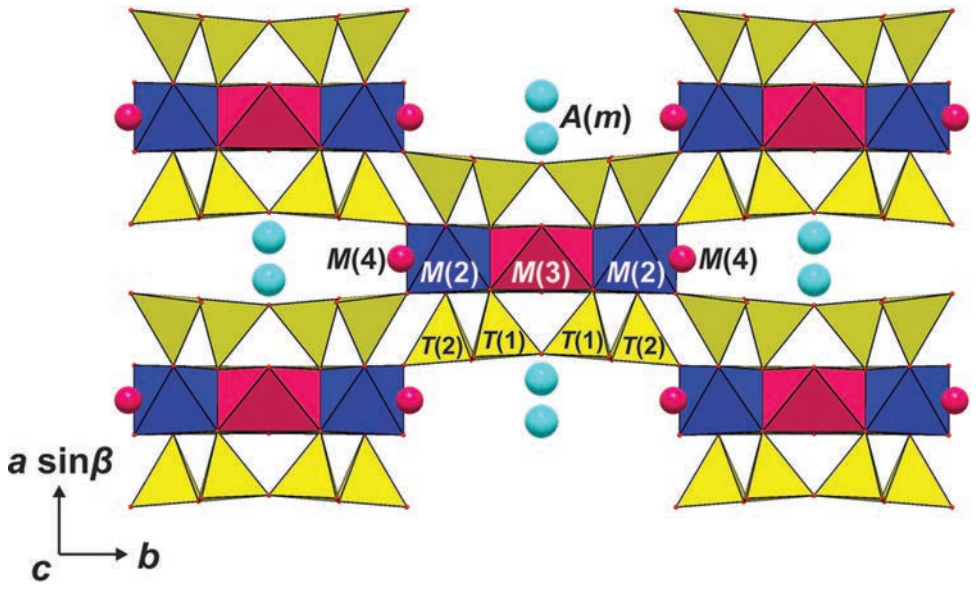

Fig. 5. The crystal structure of ferro-pedrizite: projection onto (001). (online version in colour)

In ferro-pedrizite the smallest *M*(2)-octahedron (Table 5) is occupied predominantly with Al. Minor amounts of Fe^{3+} complete the number of cations at the *M*(2) site to 2 pfu. The remaining Fe^{3+} is concentrated along with Mg in the *M*(1)-octahedron, which is smaller than the *M*(3)-octahedron. Fe^{2+} is distributed between the *M*(1) and *M*(3) sites.

Based on the refined site-scattering factors, chemical and Mössbauer data, the crystal chemical formula can be written as follows ($Z = 2$): $^{A}(Na_{0.60}K_{0.02})$ $^{M(4)}(Li_{1.89}Na_{0.07}Ca_{0.04})$ $^{C}[^{M(1)}(Mg_{0.90}Fe^{2+}_{0.75}Fe^{3+}_{0.35})^{M(2)}$ $(Al_{1.88}Fe^{3+}_{0.12})^{M((3)}(Li_{0.65}Fe^{2+}_{0.28}Mn_{0.07})]^{T}[Si_{7.79}Al_{0.21}$ $O_{22}]^{W}[(OH)_{1.36}F_{0.49}O_{0.15})]$.

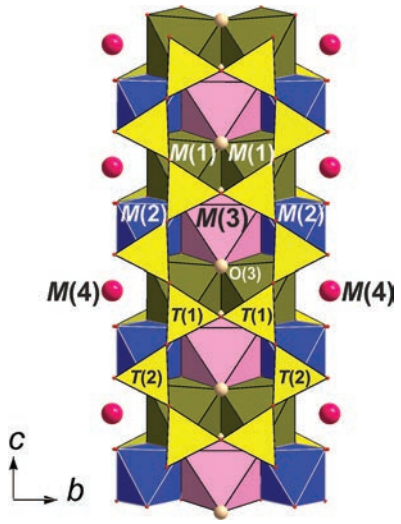

Fig. 6. The relationship between the strip of *M*(1–3) octahedra (populated by C cations) and the double-chain of *T*(1–2) tetrahedra (populated by T cations) in ferro-pedrizite. (online version in colour)

Discussion

In the Sutlug pegmatite field characterized in this paper, ferro-pedrizite is a common amphibole in endocontact zones of spodumene pegmatite veins. Apparently, it is present in numerous rare-metal pegmatite veins formed under severe tectonic conditions. The mineral crystallized during pegmatite transformation accompanied by fluorine removal into hosting carbonate rocks and by simultaneous supply of Mg from outside. In this case fluoro-pedrizite is most frequently formed at some distance from veins in hosting marbles like that in Tastyg (Oberti *et al.*, 2005), and ferro-fluoro-pedrizite is formed near the contact, as is the case in the Sutlug occurrence (Oberti *et al.*, 2009).

Volatile components of the primary fluid are preserved as inclusions in some minerals of marginal zones of the veins. According to the available data, this fluid (enriched in HCO^{-}_{3}, N_2, methane and heavier hydrocarbons) had a low water content and an extremely reducing nature (Konovalenko *et al.*, 2000; Kuznetsova & Prokofyev, 2011).

During the metasomatic stage, the system became open and the process of pegmatite transformation developed under tectonic conditions promoting the influx of more oxidizing fluids. Presumably, this explains the presence of ferric iron and of an oxo component in the group of *W*-anions of ferro-pedrizite.

Comparative data for ferro-pedrizite and other approved lithium amphiboles with the root-name ''pedrizite'' are given in Tables 6 and 7. Other amphiboles with the root-name ''pedrizite'' (pedrizite, ferri-fluoro-pedrizite, ferro-ferri-fluoropedrizite) still have to be found and characterized.

Table 6. Site populations in ferro-pedrizite and the other known amphiboles with the rootname pedrizite.

	A	B	C			T	W	
Mineral	*A*(*m*)	*M*4	*M*1	*M*2	*M*3	*T*(1) + *T*(2)	O3	Reference
Ferro-pedrizite	$Na_{0.60}K_{0.02}$	$Li_{1.89}Na_{0.07}Ca_{0.04}$	$Mg_{0.90}Fe^{2+}_{0.75}Fe^{3+}_{0.35}$	$Al_{1.88}Fe^{3+}_{0.12}$	$Li_{0.65}Fe^{2+}_{0.28}Mn_{0.07}$	$Si_{7.79}Al_{0.21}$	$OH_{1.36}F_{0.49}O_{0.15}$	This work
Ferri-pedrizite	$Na_{0.52}K_{0.04}$	$Li_{1.70}Na_{0.25}Ca_{0.05}$	$Mg_{1.49}Fe^{2+}_{0.51}$	$Fe^{3+}_{1.64}Al_{0.21}Ti_{0.09}Fe^{2+}_{0.05}$	$Li_{0.64}Fe^{2+}_{0.29}Mn_{0.07}$	Si_8	$OH_{1.31}F_{0.69}$	Caballero *et al.* (2002)
Ferro-ferri-pedrizite	$Na_{0.53}K_{0.03}$	$Li_{1.90}Na_{0.08}Ca_{0.02}$	$Mg_{1.00}Fe^{2+}_{1.00}$	$Fe^{3+}_{1.55}Al_{0.21}Ti_{0.13}Zn_{0.01}Fe^{2+}_{0.10}$	$Li_{0.58}Mn^{2+}_{0.07}Fe^{2+}_{0.35}$	Si_8	$OH_{1.45}F_{0.52}$	Oberti *et al.* (2003)
Fluoro-pedrizite	$Na_{0.64}K_{0.01}$	$Li_{1.93}Ca_{0.04}Na_{0.03}$	$Mg_{1.69}Fe^{2+}_{0.31}$	$Al_{1.98}Cr_{0.01}Zn_{0.01}$	$Li_{0.64}Fe^{2+}_{0.21}Mg_{0.13}Mn_{0.02}$	$Si_{7.96}Al_{0.04}$	$F_{1.10}OH_{0.90}$	Oberti *et al.* (2005)
Ferro-fluoro-pedrizite	$Na_{0.68}$	$Li_{1.91}Na_{0.05}Ca_{0.03}$	$Mg_{1.11}Fe^{2+}_{0.87}Zn_{0.02}$	$Al_{1.97}Fe^{2+}_{0.02}Ti_{0.01}$	$Li_{0.66}Fe^{2+}_{0.26}Mn_{0.08}$	$Si_{7.98}Al_{0.02}$	$F_{1.03}OH_{0.97}$	Oberti *et al.* (2009)

Table 7. Comparative data for ferro-pedrizite and the other known amphiboles with the rootname pedrizite.

Mineral	Ferro-pedrizite	Ferri-pedrizite	Ferro-ferri-pedrizite	Fluoro-pedrizite	Ferro-fluoro-pedrizite
End-member formula	$NaLi_2(Fe^{2+}{}_2Al_2Li)Si_8O_{22}(OH)_2$	$NaLi_2(MgFe^{3+}{}_2Li)Si_8O_{22}(OH)_2$	$NaLi_2(Fe^{2+}{}_2Fe^{3+}{}_2Li)Si_8O_{22}(OH)_2$	$NaLi_2(Mg_2Al_2Li)Si_8O_{22}F_2$	$NaLi_2(Fe^{2+}{}_2Al_2Li)Si_8O_{22}F_2$
Space group	*C2/m*	*C2/m*	*C2/m*	*C2/m*	*C2/m*
a, Å	9.3716	9.501	9.462	9.368	9.3720
b, Å	17.649	17.866	17.898	17.616	17.6312
c, Å	5.2800	5.292	5.302	5.271	5.2732
β, °	102.22	102.17	101.88	102.38	102.247
V, Å^3	853.5	878.1	878.6	849.6	851.5
Strong lines of the powder X-ray diffraction pattern: *d*, Å (*I*, %)	8.147 (52)	8.251 (30)	8.241 (100)*	8.120 (75)*	8.146 (100)
	4.420 (22)	3.050 (100)	4.471 (33)*	4.404 (66)*	4.430 (70)
	3.009 (100)	2.747 (30)	3.416 (39)*	3.375 (50)*	3.383 (40)
	2.7102 (28)	2.711 (40)	3.050 (60)*	3.005 (83)*	3.008 (80)
	2.6865 (29)	1.642 (40)	2.714 (72)*	2.873 (31)*	2.686 (90)
	2.4824 (19)	1.394 (30)	2.494 (36)*	2.679 (100)*	2.485 (60)
	1.6236 (21)		2.164 (23)*	2.483 (55)*	2.199 (30)
Optical data:					
α	1.614	1.695	The mean index of refraction is	1.610	1.642
β	1.638	1.700		1.627	1.644
γ	1.653	1.702	1.710*	1.633	1.652
Optical sign, 2*V*, °	(–) 75	(+) 55		(–) 55–61	(+) 68
Density, g cm^{-3}	3.13	3.15	3.24*	3.00	3.116*
	3.135*	3.19*		3.05*	
References	This work	Caballero *et al.* (2002)	Oberti *et al.* (2003)	Oberti *et al.* (2005); Ginzburg (1965)	Oberti *et al.* (2009)

*Calculated data.

Acknowledgements: This work was financially supported by the Russian Foundation for Basic Research (grant no. 14-05-00190-a). S.M.A is grateful for financial support by the Foundation of the President of the Russian Federation (grant no. MK-4990.2014.5).

References

Bakhtin, A.I. (1978): Absorption spectra of iron ions in arfvedsonites. *Zap. Vsesoyuz. Mineral. Obshch.*, **107**, 369–376. (in Russian)

Caballero, J.M., Oberti, R., Ottolini, L. (2002): Ferripedrizite, a new monoclinic ^{B}Li amphibole end-member from the Eastern Pedriza Massif, Sierra de Guadarrama, Spain, and a restatement of the nomenclature of Mg-Fe-Mn-Li amphiboles. *Am. Mineral.*, **87**, 976–982.

Chukanov, N.V. (2014): Infrared spectra of mineral species: extended library. Springer-Verlag GmbH, Dordrecht–Heidelberg–New York–London, 1716 p.

Della Ventura, G., Iezzi, G., Redhammer, G.J., Hawthorne, F.C., Scaillet, B., Novembre, D. (2005): Synthesis and crystal-chemistry of alkali amphiboles in the system Na_2O-MgO-FeO-Fe_2O_3-SiO_2-H_2O as a function of $f\,O_2$. *Am. Mineral.*, **90**, 1375–1383.

Gainov, R.R., Dooglav, A.V., Vagizov, F.G., Pen'kov, I.N., Golovanevskiy, V.A., Orlova, A.Yu., Evlampiev, I.A., Klekovkina, V.V., Klingelhöfer, G., Ksenofontov, V., Mozgova, N.N. (2013): NQR/NMR and Mössbauer spectroscopy methods: potentials and versatility in geochemical studies. *Eur. J. Mineral.*, **25**, 569–578.

Gainov, R.R., Vagizov, F.G., Golovanevskiy, V.A., Ksenofontov, V.A., Klingelhöfer, G., Klekovkina, V.V., Shumilova, T.G., Pen'kov, I.N. (2014): Application of ^{57}Fe Mössbauer spectroscopy as a tool for mining exploration of bornite (Cu_5FeS_4) copper ore. *Hyperfine Interact.*, **226**, 51–55.

Ginzburg, I.V. (1965): Holmquistite and its structural variety clinoholmquistite. *Trudy Mineral. Muz. Akad. Nauk SSSR*, **16**, 73–89. (in Russian)

Hawthorne, F.C., Oberti, R., Harlow, G.E., Maresch, W.V., Martin, R.F., Schumacher, J.C., Welch, M.D. (2012): IMA report: nomenclature of the amphibole supergroup. *Am. Mineral.*, **97**, 2031–2048.

Ibers, J.A. & Hamilton, W.C. Eds (1974): *International Tables for X-Ray Crystallography*. Vol. **IV**, The Kynoch Press, Birmingham, UK, 377 p.

Iezzi, G., Cámara, F., Oberti, R., Della Ventura, G., Pedrazzi, G., Robert, J.-L. (2004): Synthesis, crystal structure and crystal chemistry of ferri-clinoholmquistite, $\square Li_2Mg_3Fe^{3+}{}_2Si_8O_{22}(OH)_2$. *Phys. Chem. Minerals*, **31**, 375–385.

Ishida, K. & Hawthorne, F.C. (2001): Assignment of infrared OH-stretching bands in manganoan magnesio-arfvedsonite and richterite through heat-treatment. *Am. Mineral.*, **86**, 965–972.

Klingelhöfer, G., Bernhardt, B., Foh, J., Bonnes, U., Rodionov, D., de Souza, P.A., Schröder, Ch., Gellert, R., Kane, S., Gütlich, P., Kankeleit, E. (2002): The miniaturized mössbauer spectrometer MIMOS II for extraterrestrial and outdoor terrestrial applications: a status report. *Hyperfine Interact.*, **371**, 144–145.

Konovalenko, S.I. & Garmayeva, S.D. (2012): Mineralogy features and geochemical specifics of the Tastygskaya spodumene pegmatite vein series in the Southern pegmatite belt of Sangilen in Tyva. *Mineral Geochem. Mineral Res. Asia*, Tomsk TsNTI, Tomsk, **2**, 129–138.

Konovalenko, S.I., Sazontova, N.A., Naumov, V.B. (2000): Composition of the fluid in gas-liquid inclusions in spodumene pegmatite quartz. *Ore Deposits. Mineral. Geochem.* Tomsk State University, Tomsk, **2**, 57–70.

Kuznetsova, L.G. & Prokofyev, V.Yu. (2011): Geochemical features of low-fluoride lithium pegmatite fluids in the Sangilen Upland. Proceedings of the scientific conference ''Granites and ore formation processes''. IGEM RAN, Moscow, 76–77.

Kuznetsova, L.G. & Shokalsky, S.P. (2011): Lithium position in rare-metal pegmatites of the Republic of Tyva. *in Lithium of Russia. Mineral resources, innovation technologies, environmental safety. Proceedings of the All-Russia Scientific-Practical Meeting*. Publishing House of the Siberian department of the Russian Academy of Sciences, Novosibirsk, 65–70.

Mottana, A. & Griffin, W.L. (1986): Crystal chemistry of two coexisting K-richterites from St. Marcel (Val d'Aosta, Italy). *Am. Mineral.*, **41**, 1426–1433.

Oberti, R., Cámara, F., Caballero, J.M., Ottolini, L. (2003): Sodic-ferri-ferropedrizite and ferri-clinoferroholmquistite: mineral data and degree of order in the *A*-site cations in Li-rich amphiboles. *Can. Mineral.*, **41**, 1345–1354.

Oberti, R., Cámara, F., Ottolini, L. (2005): Clinoholmquistite discredited: the new amphibole end-member fluoro-sodic-pedrizite. *Am. Mineral.*, **90**, 732–736.

Oberti, R., Hawthorne, F.C., Cannillo, E., Cámara, F. (2007): Long-range order in amphiboles. *Rev. Mineral. Geochem.*, **67**, 125–171.

Oberti, R., Boiocchi, M., Ball, N.A., Hawthorne, F.C. (2009): Fluoro-sodic-ferropedrizite, $NaLi_2(Fe^{2+}{}_2Al_2Li)Si_8O_{22}F_2$, a new mineral of the amphibole group from the Sutlug River, Tyva Republic, Russia: description and crystal structure. *Mineral. Mag.*, **73**, 487–494.

Oxford Diffraction (2009): CrysAlisPro. Oxford Diffraction Ltd, Abingdon, Oxfordshire, UK.

Petricek, V., Dusek, M., Palatinus, L. (2006): Jana2006. Structure determination software programs. Institute of Physics, Praha, Czech Republic.

Received 20 November 2014
Modified version received 1 February 2015
Accepted 2 February 2015